Temperature dependence of the Raman spectrum of $Al_xGa_{1-x}As$ ternary alloys

J. Jiménez,* E. Martín, and A. Torres
Física de la Materia Condensada, ETS Ingenieros Industriales, 47011 Valladolid, Spain

J. P. Landesman
THOMSON CSF, Laboratoire Central de Recherche, Domaine de Corbeville, 91404 Orsay, France
(Received 3 February 1998; revised manuscript received 1 June 1998)

We have studied the effect of the temperature on the first-order Raman spectra of $Al_xGa_{1-x}As$ alloys. The temperature induced frequency shift is studied over the full composition range between 300 and 650 K. It is found that the frequency temperature coefficient, $d\omega/dT$, is higher for AlAs-like modes than for GaAs-like modes and it increases with x. Linewidth and frequency shift data were analyzed in terms of anharmonicity, thermal expansion, and cation dilution. Anharmonicity was found to be the dominant term in the variation of the temperature dependence of the frequency of AlAs modes for different alloy compositions, while thermal expansion has a high influence on GaAs modes. The linewidth data are interpreted in terms of the contribution to the Raman spectrum of phonons with $\mathbf{q}\neq 0$ and cation dilution. [S0163-1829(98)07339-1]

I. INTRODUCTION

The Raman spectrum of solids is highly sensitive to the lattice temperature.[1] This allows us to use Raman spectroscopy as a temperature probe. Furthermore, the availability of Raman microprobes opens the possibility of using Raman scattering as a contactless local temperature probe with submicrometer spatial resolution. A potential application of the Raman microprobe is the local temperature assessment of power devices under operation.[2,3] This is a crucial issue, since heating limits the maximum output power, and it is one of the main causes for device failure. In particular, local temperatures have been measured in the mirror facets of biased laser diodes using a Raman microprobe.[3–5] Usually, this measurement is done by means of the Stokes/antiStokes intensity ratio.[6] Potentially, the other Raman parameters, frequency and linewidth, can provide the same information with higher experimental simplicity and accuracy. The use of frequency and linewidth demands a previous knowledge of the evolution of these parameters with the temperature for the material under study. This information is available for materials such as silicon, for which a huge body of literature has described the temperature behavior of the Raman spectrum from low temperature to melting.[1,7–9] This is not the case for III-V compounds, for which only some reports exist.[10–13] Less information exists for ternary and quaternary alloys, which are basic materials for many power devices. To the best of our knowledge, there are no reports covering temperature ranges above 300 K, nor systematic studies about the temperature dependence of the Raman parameters with the alloy composition. $Al_xGa_{1-x}As$ is one of the main compounds for different devices, such as laser diodes and herostructure-based transistors. Thus, the study of the temperature dependence of the Raman parameters of these alloys presents a high interest for understanding their vibrational properties and the assessment of the thermal dissipation on devices based on these materials. The Raman spectrum of $Al_xGa_{1-x}As$ ternary alloys displays two mode behavior over the full composition range.[14,15] It exhibits two AlAs-like Raman bands, LO_1 and TO_1, and two GaAs-like bands, LO_2 and TO_2, respectively.

We present herein a study of the temperature induced changes in the first-order Raman modes of $Al_xGa_{1-x}As$ over the full composition range in the temperature interval 300–650 K. We show that the thermally induced frequency shift increases moderately with x, and that such a shift is more important for AlAs-like modes than for GaAs-like modes. The analysis of these data is presented in terms of thermal expansion, phonon-phonon interactions (anharmonic coupling), and cation dilution.

II. EXPERIMENT

$Al_xGa_{1-x}As$ alloy samples were grown by molecular-beam epitaxy (MBE) on (100)-oriented undoped GaAs substrates. The composition was measured by x-ray diffraction and confirmed by Raman spectroscopy.[14] Samples with five different compositions, $x=0.2$, 0.45, 0.58, 0.73, and 0.82, were studied. Bulk GaAs samples were cut from undoped (100) liquid encapsulated Czochralski (LEC) wafers. The samples were mounted on a heater stage (Mettler FP82 HT). The temperature range explored was 300–650 K with an accuracy better than 0.1 °C.

Raman spectra were recorded in backscattering configuration with a DILOR X-Y Raman spectrometer attached to a metallographic microscope (Olympus BHT). Multichannel detection was done with a liquid-nitrogen-cooled charge-coupled device (CCD). The Raman spectra were recorded after a stabilization time long enough to avoid temperature fluctuations. The excitation was done with the 514.5-nm line of an Ar+ laser, the laser power density was below 100 kW/cm^2. The incident laser beam was polarized parallel to crystallographic axes $\langle 100\rangle$ for (001) surfaces and $\langle 110\rangle$ for (110) surfaces, while the scattered light was not systematically analyzed. All of the spectra were obtained with a high signal/noise ratio; the spectral resolution was 2 cm^{-1}. They were numerically fitted, which allowed a frequency peak uncertainty better than 0.2 cm^{-1}.

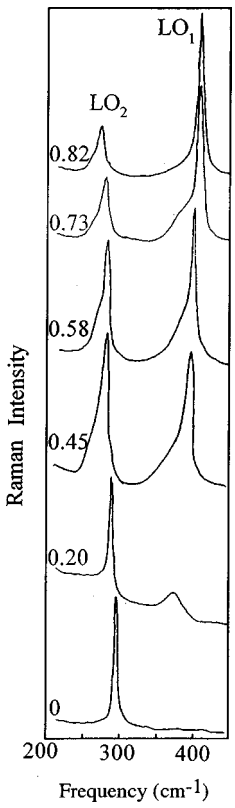

FIG. 1. Raman spectra (plane 100) for different alloy compositions.

III. RESULTS AND DISCUSSION

Typical Raman spectra for different alloy compositions and the reference bare GaAs substrate are shown in Fig. 1. An example of fitting is shown in Fig. 2. The LO modes were obtained on (100) surfaces, while cleaved (110) surfaces exhibited in some of the samples backscattering leakage and the four modes, LO_1, LO_2, TO_1, and TO_2, were observed simultaneously. The peak wave number and their relative intensities are determined by the alloy composition.[13,14] Composition and room-temperature peak frequencies are given in Table I. An example of the Raman spectra obtained at different temperatures is shown in Fig. 3.

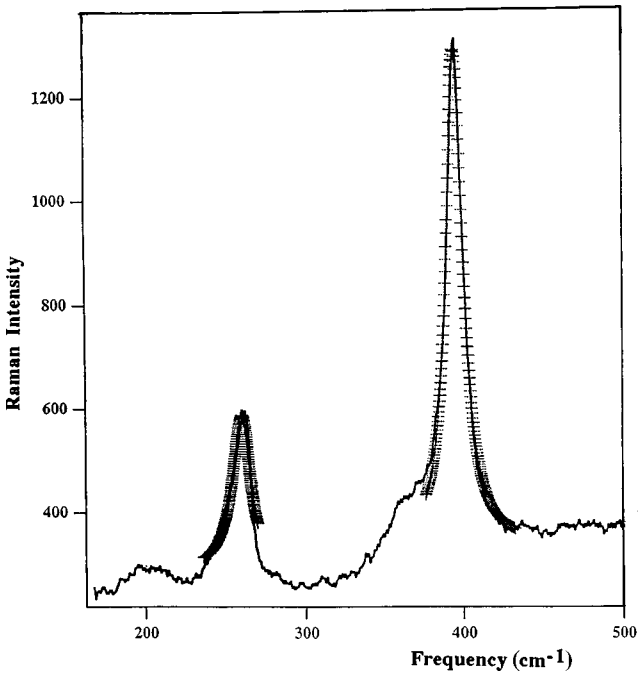

FIG. 2. Example of fitting, experimental (full line), calculated (+).

TABLE I. Room temperature wave numbers of the Raman bands TO_1, LO_1 (AlAs like), and TO_2 and LO_2 (GaAs like).

Composition (x)	LO_1 (cm^{-1})	TO_1 (cm^{-1})	LO_2 (cm^{-1})	TO_2 (cm^{-1})
0.00			293.8	270.3
0.20	368.8		283.7	271.0
0.45	284.2	356.7	272.9	262.4
0.58	388.2		271.3	
0.73	294.3	360.6	266.4	259.4
0.82	397.5	361.7	263.4	249.6

The peak frequencies of the different Raman modes are represented as a function of the temperature in Figs. 4 and 5. The frequency shift with temperature was nearly linear in the studied temperature range (best fit by least squares with $r > 0.95$). The slope, $d\omega/dT$, of these plots is represented as a function of x in Fig. 6. The temperature coefficients, $d\omega/dT$, lie in a narrow margin for all the compositions; however, a slight increase with x is observed for all the modes and such an increase is larger for AlAs like modes. Such a behavior is reported in Fig. 7 for the sample with a composition $x = 0.82$, for which the four first-order Raman modes were obtained simultaneously on a cleaved (110) surface of a thick film (2 μm) grown along the $\langle 001 \rangle$ crystal axis. Also, the temperature coefficient, $d\omega/dT$, is higher for longitudinal than for transverse modes.

The temperature dependence of the Raman peak shift has been successfully described by perturbation models.[1,7,16] Following this, the peak frequency of the i mode can be expressed as a function of the temperature[1] as

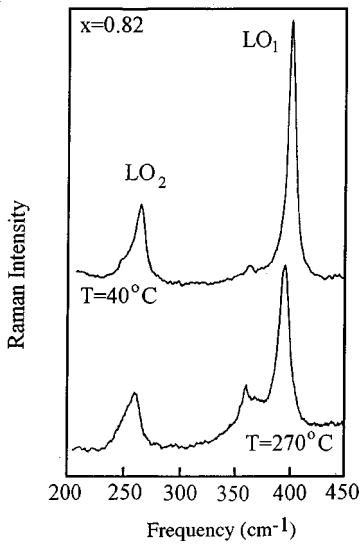

FIG. 3. Raman spectra at 40 and 270 °C.

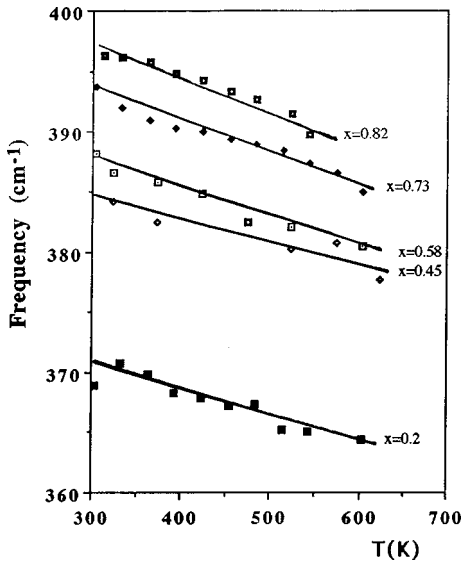

FIG. 4. Frequency vs T for LO_1 (AlAs-like) Raman band.

$$\Delta\omega_i=\omega_{oi}\left[\exp\left(-3\gamma_i\int_{To}^{T}\alpha(T')dT'\right)-1\right]+A_{1i}\left(1+\sum_{j=1}^{2}\frac{1}{e^{xj}-1}\right)+\text{higher-order terms},\tag{1}$$

where ω_{oi} is the harmonic frequency of the i mode; γ_i is the corresponding mode Gruneisen parameter ($\gamma_i=-d\ln\omega_i/d\ln V=(1/\omega_i\beta)d\omega_i/dp$, where β is the compressibility, and V and p are the volume and pressure, respectively), α the linear thermal expansion coefficient, A_{1i} the cubic anharmonic constant of mode i, and

$$\sum_{j=1}^{2}x_j=\frac{h\omega_{oi}}{KT}.\tag{2}$$

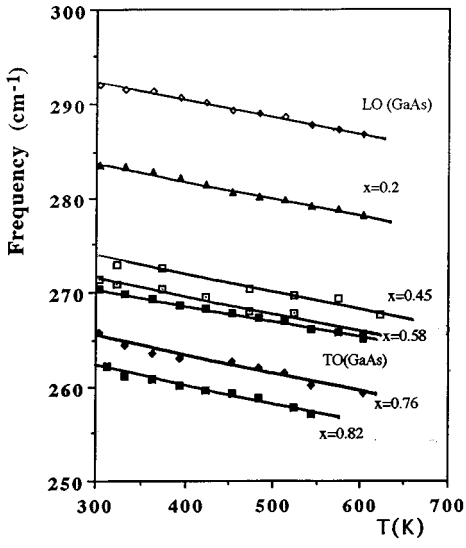

FIG. 5. Frequency vs T for LO_2 (GaAs-like) Raman band. The wave number of the TO and LO bands of GaAs are also plotted.

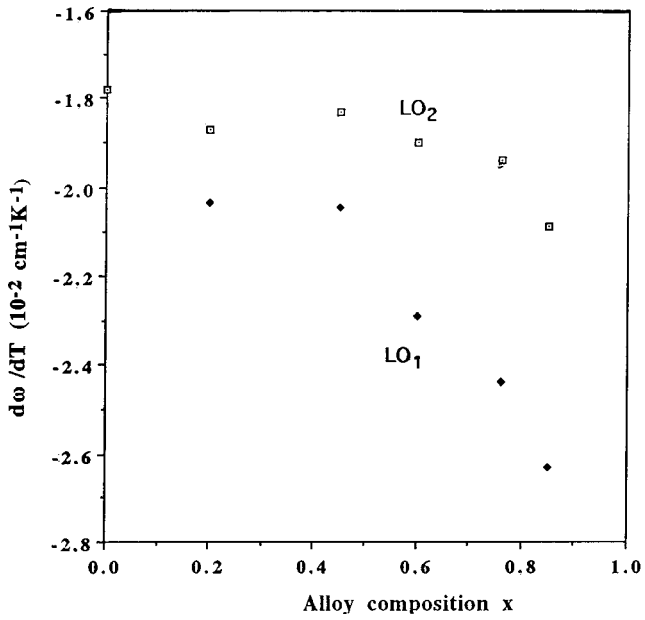

FIG. 6. Temperature coefficients ($d\omega/dT$) for LO1 (AlAs-like) and LO2 (GaAs-like) modes as a function of the alloy composition.

The first term of Eq. (1) corresponds to the thermal expansion contribution; it depends on the alloy composition and mode polarization, since γ_i and ω_{oi} are different for each mode and alloy composition and α is a function of the alloy composition.[15] The second term accounts for the cubic anharmonic phonon coupling (three phonon processes); the higher-order terms are quartic (four phonon processes) and higher anharmonic contributions. In GaAs the zone center optic phonons decay in two longitudinal acoustic (LA) phonons with energy half of the optical phonon and wave vectors $\mathbf{q}$ and $-\mathbf{q}$, respectively,[10,12] which was assumed in our calculations as well. The contribution of high-order (quartic and above) anharmonic terms was found negligible within the experimental uncertainty in the temperature range studied.

The linewidth analysis is more difficult to achieve since different contributions have to be considered. Among these, the finite resolution of the spectrometer,[13] the disorder inher-

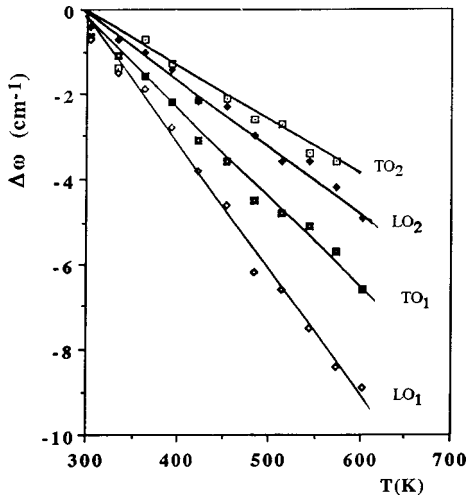

FIG. 7. Frequency shift vs T for the four Raman bands (TO_1, LO_1, TO_2, and LO_2) ($x=0.82$).

ent to the alloy[15,16] and the broadening due to the anharmonic decay of phonons. The finite resolution of the spectrometer demands a correction of the measured linewidth. The alloy potential fluctuations induce asymmetric Raman line broadening;[17,18] *a priori*, such a broadening is independent of the temperature. Besides, it is well known that the alloy disorder depends on the experimental conditions during growth.[18] The pure anharmonic broadening is a temperature dependent effect through the phonon occupation number. All these points make difficult the assessment of the linewidth data, which are more scattered than the frequency shift data.

The anharmonic broadening can be written according to the perturbation theory as:[7–10,12]

$$\Gamma_i(T)=\Gamma_{oi}+B_{1i}\left(1+\sum_{j=1}^{2}\frac{1}{e^{xj}-1}\right)+\text{higher-order terms}, \quad (3)$$

where Γ_{oi} is the harmonic linewidth independent of the temperature and B_{1i} is the corresponding cubic anharmonic constant.

The anharmonic decay of phonons can be enhanced by defects and disorder. Verma *et al.*[13] demonstrated that P^+ implanted GaAs exhibited higher anharmonic constant than the bare GaAs substrate. Also, the anharmonicity was found to vary with the composition in $In_{1-x}Ga_xP$.[19] Brafman and Manor[20] observed differences between the effects due to alloying and those produced by ion implantation. Also, the relaxation of the momentum conservation rule, which is not considered in ideal random element isodisplacement (REI) models[21] and residual stresses can contribute to the peak broadening. It follows that the linewidth has to be studied with extreme caution in order to obtain reliable anharmonic constants and temperature coefficients, $d\Gamma/dT$.

The GaAs-like LO phonon band was significantly broader than the AlAs-like LO Raman peak for samples with $x=0.45$, 0.58, 0.73, and 0.82; also GaAs-like LO modes were also more asymmetric. These data are summarized in Table II. It should be noted that out of the low values of x, Al diluted, the GaAs-related modes are broader than the corresponding AlAs-related mode. However, the ratio $\Gamma_{LO2}/\Gamma_{LO1}$ remains nearly constant from $x=0.45$ to $x=0.82$, Table II.

The GaAs-like LO Raman bands were not only broader than the AlAs-like bands but their asymmetry, Γ_l/Γ_h, is also more important for $x>0.45$ (where Γ_l and Γ_h are, respectively, the low- and high-frequency half-widths of the peak). When the Raman band is broadened only because of the finite phonon lifetime ($\Gamma\alpha\tau^{-1}$, where τ is the phonon lifetime) the Raman band is still Lorentzian, which was only the case for the binary compound ($x=0$). The asymmetry can be described assuming a finite phonon correlation length.[17]

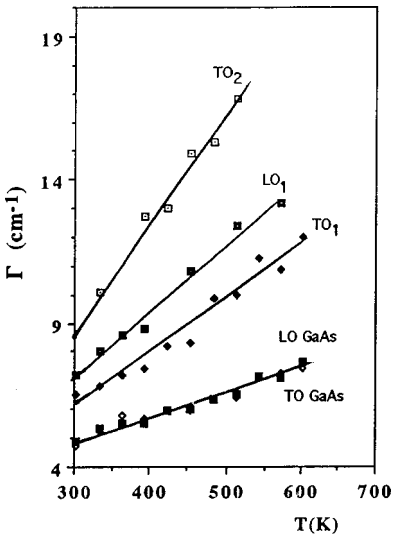

FIG. 8. FWHM vs T for TO_1, LO_1, and TO_2, Raman bands of sample $x=0.82$. FWHM vs T of TO and LO bands of GaAs are also plotted.

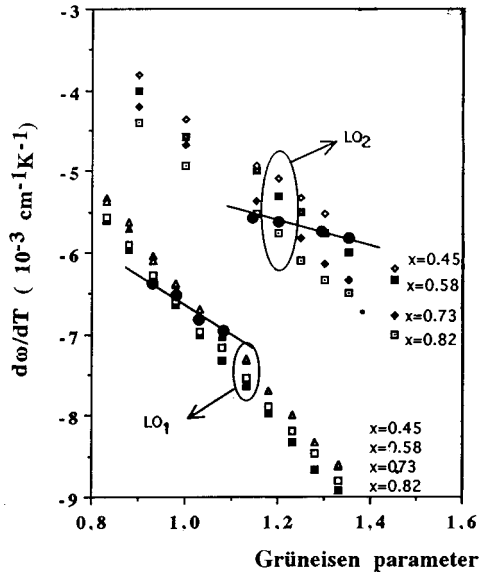

FIG. 9. Frequency shift (LO_1 and LO_2 modes) due to the thermal expansion term vs the Grüneisen parameter. The dark circles correspond to the contributions calculated for the experimental values of the Grüneisen parameters of these alloys (see text).

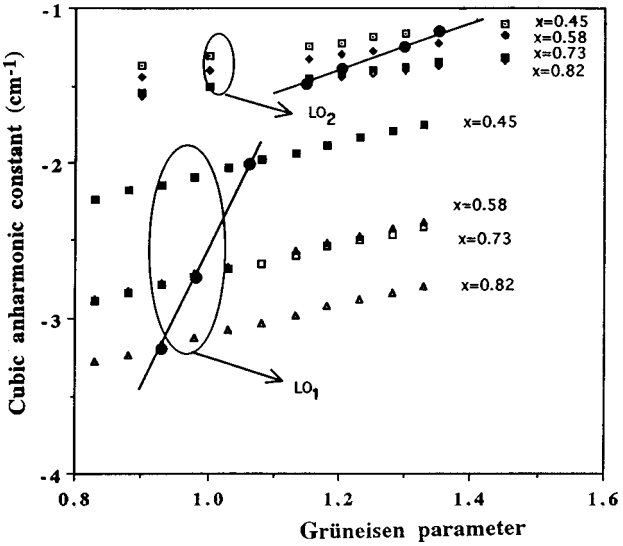

FIG. 10. Cubic anharmonic constant (LO_1 and LO_2 modes) vs the Grüneisen parameter. The dark circles correspond to the contributions calculated for the experimental values of the Grüneisen parameters of these alloys (see text).

TABLE II. Linewidths of LO_1 and LO_2 Raman peaks and relative width.

Composition (x)	Γ_{LO1} (cm^{-1})	Γ_{LO2} (cm^{-1})	$\Gamma_{LO2}/\Gamma_{LO1}$
0.20		5	
0.45	10	15	1.5
0.58	8	11	1.4
0.73	8	14	1.8
0.82	8	12	1.5

The experimental data result in a shorter correlation length for GaAs-like than for AlAs-like phonons, as it was previously reported by other authors,[18] who estimated a correlation length for LO_1 twice the correlation length of LO_2 for an alloy with $x=0.7$. However, the correlation length of phonons in ternary alloys has been the object of controversy. Kash *et al.*[22] showed that the Raman phonons in $Al_xGa_{1-x}As$ alloys have well-defined momenta, which should explain the inadequacy of a finite correlation length analysis of the Raman linewidth data. They attributed the linewidth of the first-order Raman bands of the $Al_xGa_{1-x}As$ alloy to fluctuations of the bond length that can activate forbidden $\mathbf{q}\neq 0$ phonons, which can contribute to the Raman spectrum without claiming for phonon localization.

The contribution by phonons with $\mathbf{q}\neq 0$ can be a reasonable hypothesis for describing the alloy linewidth. It should be noted that $d\omega/dq$ is larger for GaAs-like modes[17,23] than for AlAs-like modes[17,24] modes. Thus, this difference in the dispersion relation could explain the broadening features of the GaAs-like phonon compared to the AlAs like phonon.

The plots of the full width at half-maximum (FWHM) vs T of LO_1, TO_1, and TO_2 phonon modes of sample $Al_{0.82}Ga_{0.18}As$ (110) are shown in Fig. 8. LO_2 is not shown since the fitting was not good due to its weak intensity and the overlapping with TO_2. The corresponding plots for the LO and TO linewidths of a bare GaAs substrate are also represented. Noteworthy differences are observed in the corresponding temperature coefficients, $d\Gamma/dT$. The temperature coefficients are higher for GaAs-like modes than for AlAs-like modes, which suggest higher anharmonicity of GaAs-like modes, in contrast to what is expected. Besides, all these coefficients are significantly higher than those obtained for binary compound, for which only zone center phonons contribute to the Raman spectrum. The mode asymmetry, Γ_l/Γ_h, was nearly constant with T for AlAs-like modes, while, it was increasing for GaAs-like modes. However, for $x=0.2$, the asymmetry of the LO_2 mode was practically not modified by the temperature. The activation of forbidden modes (disorder-activated longitudinal optic, disorder-activated transverse optic) due to resonances does not seem to account for these observations, if we consider that the intensity of these modes comes out lower than that of the allowed modes by two orders of magnitude.[25] This behavior reinforces the role played by $\mathbf{q}\neq 0$ phonons in the Raman linewidth of the alloy modes and their dependence

TABLE III. Table summarizing pressure and temperature coefficients and Grüneisen parameters. [The pressure coefficients and the Grüneisen parameters of GaAs were obtained from Ref. 25, L. J. Cui, U. D. Venkateswaran, B A. Weinstein, and F. A. Chambers, Semicond. Sci. Technol. **6**, 469 (1991); while those of the alloy series were obtained from Ref. 26, M. Holz, M. Seon, O. Brafman, R. Manor, and D. Fekete, Phys. Rev. B **54**, 8714 (1996).]

X	Phonon mode	Pressure coefficient ($cm^{-1}\,GPa^{-1}$)	Temperature coefficient ($10^{-2}\,cm^{-1}\,K^{-1}$)	Grüneisen parameter
0.00	TO	4.38	−1.71	1.39
	LO	4.08	−1.79	1.23
0.20	LO_2		−1.87	
	LO_1		−2.03	
0.25	LO_2	4.33		1.12
	TO_1	5.10		1.15
	LO_1	5.71		1.14
0.40	LO_2	4.39		1.17
	TO_1	6.38		1.14
	LO_1	5.82		1.14
0.45	LO_2		−1.38	
	LO_1		−2.05	
0.58	LO_2	4.39	−1.90	1.22
	LO_1	6.41	−2.29	1.03
0.70	TO_2	4.08		1.30
	LO_2	4.68	−1.92	1.32
	TO_1	5.38		1.11
	LO_1	5.13	−2.40	0.97
0.82	LO_2		−2.09	
	LO_1		−2.63	
1.00	TO_1	6.40		1.22
	LO_1	5.28		0.86

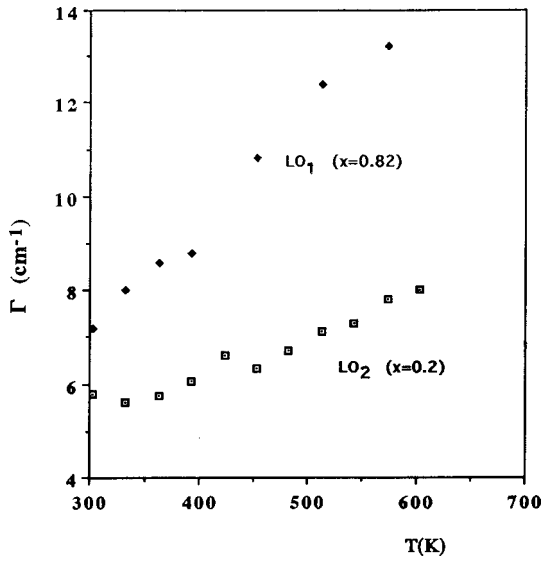

FIG. 11. FWHM vs T for LO_1 ($x=0.82$) and LO_2 ($x=0.2$) phonons.

with T. It should be noted that the anharmonic contribution to the phonon linewidth is calculated for zone center phonons in Eq. (2), which is rather probably a rough approach in the case of alloys.

The peak frequency shift was analyzed in terms of the thermal expansion and the anharmonic contribution. In order to estimate how the alloy composition can influence both contributions, Grüneisen parameters between 0.8 and 1.4 were considered. This choice was done on the bases of the experimental data concerning the Grüneisen parameters of the binary compounds [$\gamma_{LO}=1.23$ and $\gamma_{TO}=1.39$ for GaAs (Ref. 26) and $\gamma_{LO}=1.03$ and $\gamma_{TO}=1.39$ for AlAs (Refs. 27 and 28)] and those deduced from pressure measurements on $Al_xGa_{1-x}As$ alloys.[29] Then, the contribution of the thermal expansion to the frequency shift was calculated for each Raman mode and alloy composition. The experimental data were fitted by Eq. (1) assuming different Grüneisen parameters, allowing thus the estimation of the anharmonic constants. These results are summarized in Figs. 9 and 10. Both the thermal expansion contribution and the anharmonic constants vary almost linearly with γ. The variation of both with x for a given γ presents different characteristics for AlAs and GaAs-like modes. In fact, the anharmonic constant exhibits strong variations with x for AlAs modes when compared to the variation of GaAs modes; such a variation is about six times higher for AlAs- than for GaAs-like modes. Concerning the thermal expansion contribution the GaAs modes present a stronger variation with x than the AlAs modes. All that suggests that the increase of the temperature coefficient with x for AlAs-like modes is mainly the consequence of the higher anharmonicity of these modes as compared to GaAs-like modes. This can be associated in a first approximation with the smaller reduced mass of AlAs compared to GaAs.[30] Data corresponding to our sample compositions are indicated by dark circles in Figs. 9 and 10, using the Gruneisen parameters determined by Holz *et al.*[29] Table III summarizes the main data concerning pressure and temperature coefficients and the Grüneisen parameters over the full composition range.

Following the above results, the high temperature coefficients deduced from the linewidth of the GaAs-like modes can hardly be associated with an increase of the anharmonicity; therefore, it seems that the contribution by $\mathbf{q}\neq 0$ phonons is the main cause for the observed linewidth broadening. This was confirmed by the comparison between the evolution with the temperature of the FWHM's of LO_1 and LO_2 modes in the same cation dilution conditions. The FWHM's of LO_1 and LO_2 are plotted in Fig. 11 as a function of the temperature for $x=0.2\,(LO_2)$ and $x=0.82\,(LO_1)$. The temperature coefficient, $d\Gamma/dT$, is significantly higher for LO_1 than for LO_2. It can be argued that the linewidth of the Raman mode related to the most abundant cation (Ga for $x=0.2$ and Al for $x=0.82$) in low dilution conditions is mainly determined by the anharmonicity of zone center phonons, the contribution of the off-zone center phonons is expected to be much less important. As the composition goes to higher dilution, forbidden $\mathbf{q}\neq 0$ phonons are activated, which is observed by the Raman mode broadening. This agrees with the frequency data, which demonstrated a higher anharmonic contribution for the AlAs sublattice than for the GaAs sublattice.

IV. CONCLUSION

The temperature dependence of the first order Raman spectrum of $Al_xGa_{1-x}As$ has been studied over the full composition range. The temperature coefficient, $d\omega/dT$, increases with x and is higher for AlAs-like modes, as a consequence of their higher anharmonicity. Linewidth was demonstrated to be more complex to analyze, due to the contribution of $\mathbf{q}\neq 0$ phonons, that was determinant for the linewidth of the Raman modes. Cation dilution plays a main role in the activation of these forbidden modes. It was demonstrated that in low dilution conditions the corresponding modes approach the behavior of the binary compounds, confirming the frequency data about the higher anharmonicity of the AlAs-like compared to GaAs-like modes. AlAs-like modes are more sensitive for temperature measurements.

ACKNOWLEDGMENTS

Fruitful discussions with I De Wolf (IMEC, Leuven) and E. Da Silva (DILOR, Lille) are acknowledged. The authors are indebted to J. Nagle (Thomson CSF, Paris) for kindly supplying the samples and for a critical reading of the manuscript. This work was funded under UE Contract No. SMT-CT 95 2024.

*Author to whom correspondence should be addressed. Electronic address: jimenez@hp9000.uva.es

[1] J. Menéndez and M. Cardona, Phys. Rev. B **29**, 2051 (1985).
[2] R. Osstermeier, K. Brunner, G. A. Abstreiter, and W. Weber, IEEE Trans. Electron Dev. **39**, 858 (1992).
[3] W. C. Tang, H. J. Rosen, P. Vettiger, and D. J. Webb, Appl. Phys. Lett. **58**, 557 (1991).
[4] P. W. Epperlein, P. Buchmann, and A. Jakubowicz, Appl. Phys. Lett. **62**, 455 (1993).
[5] R. Puchert, A. Barwolff, U. Menzel, A. Lau, M. Voss, and T.

Elsaesser, J. Appl. Phys. **80**, 5559 (1996).
[6] A. Compaan and J. Trodhal, Phys. Rev. B **29**, 793 (1984).
[7] M. Balkanski, R. F. Wallis, and E. Haro, Phys. Rev. B **28**, 1928 (1983).
[8] T. R. Hart, R. L. Aggarwal, and B. Lax, Phys. Rev. B **1**, 638 (1970).
[9] H. Tang and I. P. Herman, Phys. Rev. B **43**, 2299 (1991).
[10] B. Jusserand and J. Sapriel, Phys. Rev. B **24**, 7194 (1981).
[11] J. R. Shealy and G. W. Wicks, Appl. Phys. Lett. **50**, 1173 (1987).
[12] G. Irmer, M. Wenzel, and J. Monecke, Phys. Status Solidi B **195**, 85 (1996).
[13] P. Verma, S. C. Abbi, and K. P. Jain, Phys. Rev. B **51**, 16 660 (1995).
[14] O. K. Kim and W. G. Spitzer, J. Appl. Phys. **50**, 4362 (1979).
[15] S. Adachi, J. Appl. Phys. **58**, R1 (1985).
[16] H. H. Burke and I. P. Herman, Phys. Rev. B **48**, 15 016 (1993).
[17] P. Parayanthal and F. H. Pollak, Phys. Rev. Lett. **52**, 1822 (1984).
[18] Pudong Lao, W. C. Tang, A. Madukhar, and P. Chen, J. Appl. Phys. **65**, 1676 (1989).
[19] R. Beserman, C. Hirliman, M. Balkanski, and J. Chevallier, Solid State Commun. **20**, 485 (1976).
[20] O. Brafman and R. Manor, Phys. Rev. B **51**, 6940 (1995).
[21] S. Yamazaki, A. Ushikorawa, and T. Katoda, J. Appl. Phys. **51**, 3722 (1980).
[22] J. A. Kash, J. M. Hvam, J. C. Tsang, and T. F. Kuech, Phys. Rev. B **38**, 5776 (1988).
[23] J. L. T. Waugh and G. Dolling, Phys. Rev. **132**, 2410 (1963).
[24] H. M. Kagaya and T. Soma, Solid State Commun. **48**, 785 (1983).
[25] M. Bernasconi, L. Colombo, L. Miglio, and G. Benedek, Phys. Rev. B **43**, 14 447 (1991).
[26] T. Soma, J. Satoh, and H. Matsuo, Solid State Commun. **42**, 889 (1982).
[27] P. Seguy, J. C. Mann, G. Martinez, and K. Ploog, Phys. Rev. B **40**, 8452 (1990).
[28] L. J. Cui, U. D. Venkateswaran, B. A. Weinstein, and F. A. Chambers, Semicond. Sci. Technol. **6**, 469 (1991).
[29] M. Holz, M. Seon, O. Brafman, R. Manor, and D. Fekete, Phys. Rev. **54**, 8714 (1996).
[30] D. Vanderbilt, S. G. Louie, and M. L. Cohen, Phys. Rev. B **33**, 8740 (1986).